3D Printed Porous Ceramic Implants Infiltrated with Biodegradable Biopolymer Composites for Improved Mechanical and Biofunctional Behaviour

Ernesto J. Delgado-Pujol[1]([✉]) , Gemma Fargas[2,3] , Victoria Axelrad[4] ,
Guillermo Martinez[5] , Gemma Herranz[4] , Belén Begines[5] , Cristina Berges[4] ,
Luis Llanes[2,3] , Ana Alcudia[5] , and Yadir Torres[1]

[1] Departamento de Ingeniería y Ciencia de los Materiales y del Transporte, Escuela Politécnica Superior, Universidad de Sevilla, 41011 Seville, Spain
edelgado4@us.es

[2] Departamento de Ciencia e Ingeniería de Materiales, Universidad Politécnica de Cataluña, 08019 Barcelona, Spain

[3] Centro de Investigación en Ciencia e Ingeniería Multiescala de Barcelona, Universidad Politécnica de Cataluña, 08019 Barcelona, Spain

[4] INEI-Escuela Técnica Superior de Ingeniería Industrial, Universidad de Castilla–La Mancha, 13071 Ciudad Real, Spain

[5] Departamento de Química Orgánica y Farmacéutica, Facultad de Farmacia, Universidad de Sevilla, 41012 Seville, Spain

Abstract. The incidence of fractures and bone defects has been a significant driving force behind research efforts aimed at enhancing the quality of life for patients. However, it is important to acknowledge the inherent complexities of this research field. Where each patient could have different scenarios along with the difficulty of replicate the properties and complex design of the bones. In this study, scaffolds previously manufactured by different 3D printing techniques made of ceramic materials, specifically yttria-stabilised zirconia, which has excellent biocompatibility and mechanical properties, were used. These samples, which exhibit different designs to be employed in specific medical situation, have been characterised according to his morphology and porosity; using the outcomes for select the most promising for subsequent infiltration with appropriate biopolymers in order to improve their *in vivo* performance. Specifically oriented towards improve the osseointegration capacity by adding nanohydroxyapatite (nHA). The infiltrated samples were evaluated in terms of polymer degradation inside the composite, swelling evaluation, and studies of apatite formation capacity on the surface (bioactivity) assessed through XRD.

Keywords: 3D printing · biofunctionalization · biopolymer · osteointegration · scaffold

1 Introduction

Bone possesses the remarkable ability to regenerate itself, but this regenerative capacity is limited to small micro-fractures. When faced with larger defects, surgical intervention becomes necessary for effective repair. These defects can arise from various factors, with aging being particularly prevalent due to the increasing life expectancy of the population, leaving older individuals more vulnerable to bone-related issues [1]. Bone exhibits a unique mechanical behaviour, combining elements of both brittleness and flexibility. To successfully repair bone using tissue engineering approaches, implant materials must achieve a balance in terms of their mechanical properties, which closely depend on their internal geometry and the dense-porous combination they possess [2]. Proper material selection based on specific requirements plays a crucial role in achieving desirable outcomes [3].

Zirconia emerges as a promising option for bone repair, given its widespread utilization in various industries owing to its excellent mechanical, thermal, and electrical properties. In the field of biomedical applications, particularly in dentistry, zirconia ranks among the potential materials due to its notable chemical stability, biocompatibility, and aesthetically pleasing appearance. While conventional milling methods have traditionally been used for zirconia component fabrication, 3D printing technology is now emerging as an alternative approach [4]. Additive manufacturing, also known as 3D printing, offers the advantage of producing complex geometries and enabling the design of composite structures that aim to replicate the mechanical response of the human body.

The objective of this particular study is to fabricate porous zirconia scaffolds using two specific 3D printing techniques: "Direct Ink Writing" (DIW) and "Fused Filament Fabrication" (FFF). The designs are based on a cylinder with controlled and interconnected porosity, as well as a prism with similar characteristics. By employing these advanced printing techniques, the researchers aim to create scaffolds that allow for enhanced cell adhesion, nutrient diffusion, and vascularization, promoting bone regeneration within the defects.

2 Material and Methods

The chemicals were used in the original state in which they were supplied, and no additional purification steps were performed; these were purchased from Sigma-Aldrich (Madrid, Spain) unless otherwise stated. Poly-ε-caprolactone (PCL, average molecular weight of 80,000 g/mol), polyvinyl alcohol (PVA, with molecular weights ranging from 30,000 to 70,000 g/mol and 87–90% hydrolysis), hydroxyapatite nanopowder (nHA) (<200 nm, purity ≥ 97%), and dichloromethane, the latter supplied by Honeywell in Badalona, Spain, were used for biocopolymer synthesis. The products employed during apatite formation studies (described in ISO 23317:2014) were also supplied by Sigma-Aldrich, excepting hydrochloric acid was sourced from Scharlau Lab (Barcelona, Spain). Nikon SMZ25 stereo microscope (Nikon Corporation, Tokyo, Japan) with camera device coupled driven by NIS Elements v 5.11.02, also from Nikon, were employed for image characterization. Degradation studies and the evaluation of apatite formation were conducted using an orbital shaker (Heidolph Unimax 1010) equipped with the ambient

temperature controller Heidolph Incubator 1000 (Heidolph Instruments GmbH & Co. KG, Schwabach, Germany). A Bruker D8 Advance A25 diffractometer with Cu Kα radiation (0.154 nm) characterised apatite formation for TF-RDX, while morphological evolution during the degradation study was observed using a Phenom Pro SEM. Additionally, sample weights were monitored with a Mettler AE 100 balance (Mettler Toledo, Columbus, United States).

2.1 Scaffold Manufacturing and Characterization

Two different scaffolds were manufactured using different 3D printing techniques: DIW and FFF. In both cases, the starting point was ytria-stabilised zirconia powder. The process of ink formulation for DIW and filament preparation for FFF together printing conditions has been described by the authors in previous works [5, 6]. Both 3D printed ceramic scaffolds were morphologically characterised using macro-images obtained with a magnifying glass to determine the pores and filament dimensions (Deq and Dfilament). Furthermore, the percentage of total and interconnected porosity (Pi and PT, respectively) was assessed using the Archimedes method on at least three samples from each variant.

2.2 Biopolymer Synthesis and Infiltration

The biopolymer composite synthesis has been described by the authors in previous communications [7]. Subsequently, for the infiltration process, the samples were placed into a flask and immersed in the composite. The samples were left at room temperature to evaporate the remanent dichloromethane in the mixture. Infiltrated samples were denominated using the composite ratio: 80/20-B for the reference composite without nHA, 80/20-5 for the biopolymer with a 5 wt% nHA.

2.3 Swelling Studies

Swelling studies were conducted over the biopolymeric composite in order to assess the water uptake level. The samples were soaked in PBS solution and his weight was recorded each half hour after beginning the study. After one hour of process, the measurements were made each hour until reach 6 h of study where the weight was measured in a more discrete time lapse: 24 h, 2 days, 1 month, and 2 months. For registering the weight values, the samples were removed from the PBS solution, and the excess water was gently removed.

2.4 Degradation Studies

The degradation study was conducted over the ceramic 3D printed infiltrated with the polymeric composite PCL/PVA variant. The scaffolds were placed in a flask containing 40 ml of PBS solution for 8 weeks at constant agitation of 120 rpm and temperature fixed in 37 °C. During the study, weight changes were registered weekly using a scale. Likewise, scaffolds surface was observed by SEM looking for evidence of degradation.

2.5   Apatite Formation Ability

The evaluation of apatite formation was conducted following the ISO 23317:2014. Firstly, simulated body fluid (SBF) was prepared as described in the standard. Consequently, the infiltrated samples were placed in a flask and filled with an amount of SBF solution, according to the superficial area of each specimen. The SBF solution was renewed weekly throughout the study and the temperature was maintained at $37\,^{\circ}\mathrm{C}$. After the experiment, the samples were removed from the solution, washed with distilled water, and allowed to air dry at room temperature. For apatite formation evaluation, the TF-XRD technique was employed with the samples before, during and after the experiment.

3   Results and Discussion

During the presentation and discussion of the results, a first comparison will be made between the two designs based on the results of their characterization. The chosen one will be infiltrated with the biopolymer composite and subjected to the aforementioned studies. The results obtained are presented in this section.

   The samples obtained from each 3D printing method were characterised as mentioned above. Result used to compare between both designs and choose one for the posterior infiltration process. From Fig. 1 can be said that samples meet in a high level the design proposed initially.
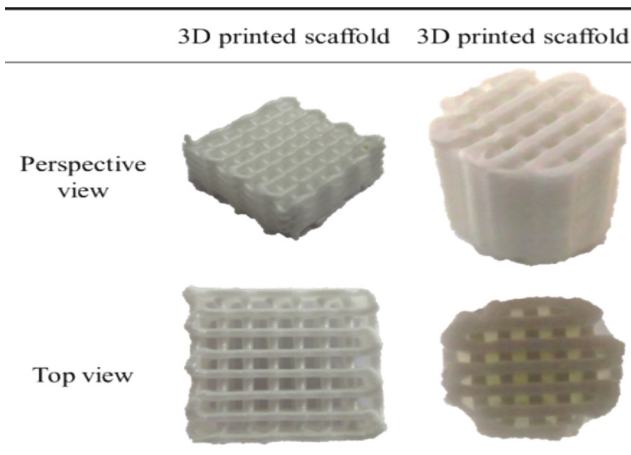

Fig. 1. Macro images of the 3D printed scaffolds manufactured by DIW (left) and FFF (right).

   From the images obtained with the stereo microscope, filament diameter and pore size were measured and are presented in Table 1. Likewise, the results of interconnected porosity and total porosity obtained by the Archimedes method are shown in the table. Although both scaffolds presented a high percentage of interconnected porosity in relation with total porosity; the prism shaped sample resulted to have a greater porosity

than de cylinder (53% against 24%). On the other hand, an inverse relation is observed for filament diameter and pore size, where cuboid sample presented thicker filament diameter and lower pore size than the cylinder.

Table 1. Results of imagen analysis and Archimedes method for morphological and porosity characterization.

Scaffold	P_T (%)	P_i (%)	$D_{filament}$ (μm)	Pore size (μm)
Cuboid	53 ± 1	52 ± 1	619 ± 35	404 ± 38
Cylinder	24 ± 2	24 ± 2	458 ± 56	513 ± 150

Regarding the characteristics of each sample the prism shaped one was selected over the cylinder for continue the study. The decision was based on the percentage of porosity and pore dimensions obtained, where this could be beneficial for vascularization and posterior bone ingrowth [8]. In addition, this morphology could be implemented for a broad range of bone defects repairing.

The infiltration process was successful, the highly porous body of the sample allowed the biopolymer to penetrate the sample. This relation of composition has been extensively described in past communications for biofunctional enhancement against bacterial colonisation; regarding previous research this combination could work in an adequate ratio of degradation allowing bone in-growth [7, 9].

Swelling study was conducted for 2 months, as result of mass evolution register Fig. 2a, b graph were made. For all variants of infiltrated scaffold an initial mass increase followed by a decrease in the next 3 h of study. From this point a slight increase was maintained for the subsequent 3 week. However, the weight measurements at 4 weeks and 8 weeks values were close. In terms of starting and ending point of the study the non-containing nHA sample showed the lower weight change, while for 80/20-5 a higher water uptake was obtained (8.51%).
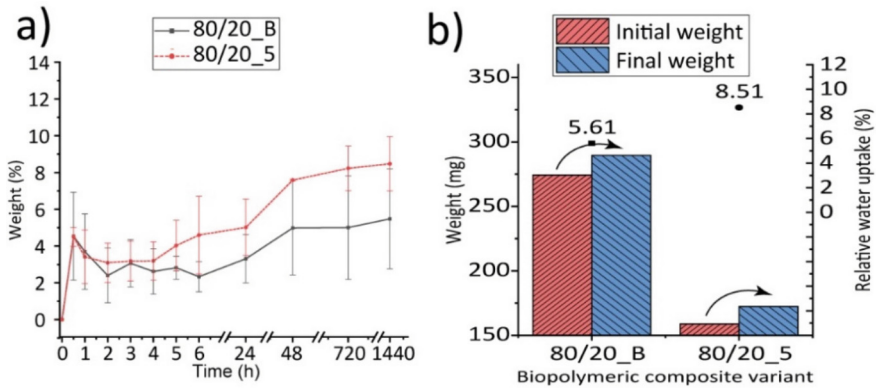
Fig. 2. Graph resulting from infiltrated scaffold characterization: a) and b) correspond to the mass variation during swelling study.

The scaffolds infiltrated with the different biopolymeric composited were subjected to degradation study for 8 weeks. Figure 3a-d shows the samples state at the study starting point and once finished of the scaffold surface. From the SEM images a few changes in the material could be noticed: such as a lower level of roughness after the degradation and higher percentage and size of existing pores. In addition, a chart using initial and final weight is represented in Fig. 1e, were the relative loss of weight values support the previous affirmation, where 80/20-B shown a reduction of 1.99% while 5 wt% nHA containing sample decreased in 3.57%.
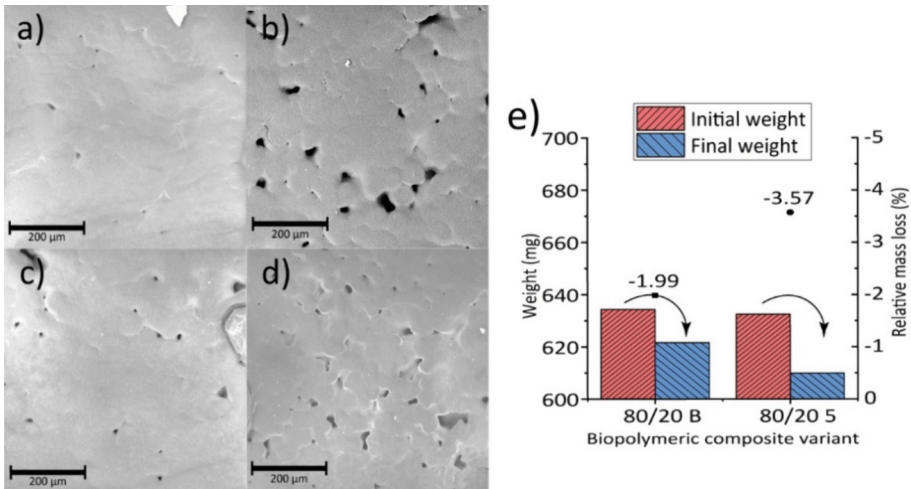

Fig. 3. SEM images a) and b) of 80/20-B variant prior and post degradation study; c) and d) SEM images of 80/20-5 variant prior and post degradation study, while and e) represent weight measurements at initial and ending point of degradation study.

XRD spectra represented in Fig. 4a, b was obtained from the non-infiltrated scaffold. The presence of peaks associated with apatite could be due to the formation and precipitation in the SBF. On the other hand, the sample which have incorporated nHA (Fig. 1b) since the initial spectra peaks associated with calcium phosphates could be identified. However, the intensity of those signals increased across the study. Therefore, this sample shown the capacity for apatite forming on their surface. The presence of this type of products on samples is usually related with bone formation capability [10, 11].
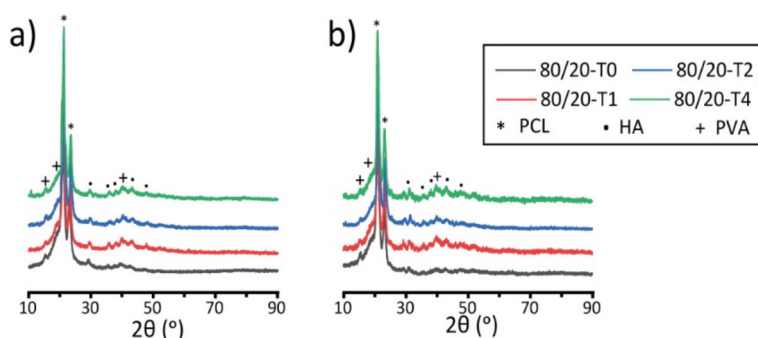

Fig. 4. XRD spectra resulting from apatite formation study for a) 80/20-B and b) 80/20-5 respectively.

4   Conclusions

The 3D printed samples were successfully fabricated and characterised. The porosity parameters of the scaffolds were very different; however, the relative interconnected porosity was above 95% in both samples. Furthermore, the range of pore size found could have a positive effect on vascularisation and allow the bone to grow inside while the infiltrated biopolymer degrades. Moreover, the swelling and apatite formation evaluation outcomes supported that 80/20-5 could have a significant effect on functionality sample. Although the prism scaffold was selected for research, the cylindrical sample is still promising and could be preferably used for large bone defects, as the morphology should be more suitable than the prism design [5].

References

1. Nauth, A., McKee, M.D., Einhorn, T.A., Watson, J.T., Li, R., Schemitsch, E.H.: Managing bone defects. J. Orthop. Trauma **25**(8), 462–466 (2011). https://doi.org/10.1097/BOT.0b013e318224caf0

2. Egol, K.A., Nauth, A., Lee, M., Pape, H.C., Watson, J.T., Borrelli Jr, J.: Bone grafting: sourcing, timing, strategies, and alternatives (in eng). J. Orthop. Trauma **29**(Suppl 12), S10–S14 (2015). https://doi.org/10.1097/bot.0000000000000460

3. Alonzo, M., et al.: Bone tissue engineering techniques, advances, and scaffolds for treatment of bone defects. Curr. Opin. Biomed. Eng. **17**, 100248 (2021). https://doi.org/10.1016/j.cobme.2020.100248

4. Elhadad, A.A., et al.: Applications and multidisciplinary perspective on 3D printing techniques: recent developments and future trends. Mater. Sci. Eng. R: Rep. **156**, 100760 (2023). https://doi.org/10.1016/j.mser.2023.100760

5. Herranz, G., et al.: Design and manufacturing by fused filament technique of novel YSZ porous grafts infiltrated with PCL/PVA/AgNPs for large bone defects repairing. J. Mater. Res. Technol. **29**, 3393–3408 (2024). https://doi.org/10.1016/j.jmrt.2024.02.057

6. Hodásová, L.U., et al.: Polymer infiltrated ceramic networks with biocompatible adhesive and 3D-printed highly porous scaffolds. Addit. Manuf. **39**, 101850 (2021). https://doi.org/10.1016/j.addma.2021.101850

7. Delgado-Pujol, E.J., et al.: Porous beta titanium alloy coated with a therapeutic biopolymeric composite to improve tribomechanical and biofunctional balance. Mater. Chem. Phys. **300**, 127559 (2023). https://doi.org/10.1016/j.matchemphys.2023.127559

8. Beltrán, A.M., Begines, B., Alcudia, A., Rodríguez-Ortiz, J.A., Torres, Y.: Biofunctional and tribomechanical behavior of porous titanium substrates coated with a bioactive glass bilayer (45S5–1393). ACS Appl. Mater. Interfaces **12**(27), 30170–30180 (2020). https://doi.org/10.1021/acsami.0c07318

9. Alcudia, A., et al.: Development of porous silver nanoparticle/polycaprolactone/polyvinyl alcohol coatings for prophylaxis in titanium interconnected samples for dental implants. Colloid Interface Sci. Commun. **48**, 100621 (2022). https://doi.org/10.1016/j.colcom.2022.100621

10. Zadpoor, A.A.: Relationship between in vitro apatite-forming ability measured using simulated body fluid and in vivo bioactivity of biomaterials. Mater. Sci. Eng. C **35**, 134–143 (2014). https://doi.org/10.1016/j.msec.2013.10.026

11. Albrektsson, T., Johansson, C.: Osteoinduction, osteoconduction and osseointegration. Eur. Spine J. **10**(2), S96–S101 (2001). https://doi.org/10.1007/s005860100282